Mutual Interference of Two Subsurface Cracks in a Semi-Infinite Body Due to Rolling Contact with Frictional Heating*

Takahito GOSHIMA**, Sotomi ISHIHARA**,
Masayoshi SHIMIZU** and Toshimichi SODA***

This paper deals with the two-dimensional thermoelastic contact problem of a rolling rigid roller of specified shape, which induced of friction and heat generation in the contact region, moving with constant velocity in an elastic half-space containing a couple of subsurface cracks. In the present temperature analysis, the speed of the moving heat source is assumed to be much greater than the ratio of the thermal diffusivity and the half contact length. The problem is solved using complex-variable techniques and is reduced to singular integral equations which are solved numerically. Numerical results of stress intensity factors are obtained for the case of two short cracks which are located parallel to the surface. The variance in interference effects on the stress intensity factors with the distance between two cracks, and the effects of the frictional coefficient, the sliding/rolling ratio and the depth of the crack location on the results are considered.

Key Words: Elasticity, Thermal Stresses, Contact Problem, Stress Intensity Factor, Subsurface Crack, Mutual Interference, Frictional Heating

1. Introduction

The rolling contact fatigue failure such as shelling in railroads, spalling in rollers, may be manifested by originating and growing subsurface cracks due to periodic rolling/sliding contact. These subsurface cracks may be initiated by preexisting defects such as inclusions, gas pores, or local soft spot, or may be generated during the cyclic straining process itself. Since the analysis for delamination theory of Suh[1], a considerable amount of research[2]-[8] on fracture mechanics has been performed in order to understand the mechanism of subsurface crack initiation and propagation in rolling/sliding contacts. These studies, however, dealt with an isothermal case. Most rolling contacts are accompanied by frictional heat generation due to the relative slip between the two contact surfaces. Goshima and coworkers[9] subsequently dealt with the thermoelastic rolling contact problem for a subsurface crack. However, multiple subsurface crack analysis under rolling/sliding contact accompanied by frictional heating has not been performed as yet. For multiple surface cracks, one of the authors[10],[11] has showed that the stress intensity factors decrease due to the mutual interference effects. Otherwise, for the case of multiple subsurface cracks, the stress intensity factors will happen to be increased due to the mutual interference effects. Therefore, it will be very important to analyze the stress intensity factors for multiple subsurface cracks under the rolling/sliding contact with frictional heating.

In this study, we analyze the stress intensity factors for a pair of subsurface cracks in an elastic half-space under rolling/sliding contact with frictional heating by a rigid roller. This thermoelastic contact is dealt with as a mixed boundary value problem with a specified displacement shape beneath the rigid roller. The crack face friction is neglected. In the present temperature analysis, it is assumed that

* Received 31st May, 2001. Japanese original: Trans. Jpn. Soc. Mech. Eng., Vol. 66, No. 648, A (2000), pp. 1489-1505 (Received 16th February, 2000)

** Faculty of Engineering, Toyama University, 3190 Gofuku, Toyama 930-8555, Japan

*** Aichi Steel Corporation, 1 Wano Wari Arao-machi, Toukai 476-0003, Japan. E-mail: goshima@eng.toyama-u.ac.jp

the speed of the moving contact region is much greater than the ratio of the thermal diffusivity to the contact length (large Peclet number), and that the temperature distribution is not disturbed by the cracks. Numerical calculations of stress intensity factors are carried out for two subsurface cracks arranged in a series or in a row which are parallel to the contact surface. The effects of the distance between cracks, the frictional coefficient, the slide/roll ratio and the subsurface depth of the cracks upon mutual interference of cracks are considered numerically.

2. Problem Formulation

An elastic half-space containing a couple of subsurface cracks is subjected to rolling/sliding contact by a rigid roller with constant velocity V, as shown in Fig. 1. The surface of the half-space is specified as the displacement shape of the roller in the contact region. We call the cracks crack 1 and crack 2 in the order of contact. In the analysis, the dimensionless parameters for crack 1 or 2 are represented by subscript k (where $k=1, 2$) and are shown as:

$$(x, y)=(\tilde{x}/c, \tilde{y}/c),\ (\xi_k, \zeta_k)=(\tilde{\xi}_k/c, \tilde{\zeta}_k/c),$$
$$l_k=\tilde{l}_k/c,$$
$$R=\tilde{R}/c,\ x_0=\tilde{x}_0/c,\ x_k=\tilde{x}_k/c,\ Y_k=\tilde{Y}_k/c,$$
$$S_r=V_s/V,\ P_e=cV/\varkappa_t,$$
$$H_0=\frac{2\alpha_0 G_0 \varkappa_t(1+\nu)}{K_t(1-\nu)},\ P_r=\frac{RP_0}{G_0}$$

Where $\varkappa_t$ is thermal diffusivity, K_t is thermal conductivity, G_0 is shear modulus, ν is Poissoin's ratio, α_0 is coefficient of thermal expansion, P_0 is the maximum contact pressure, $\tilde{x}_0$ and $\tilde{y}_0$ are the rigid displacement components of the roller, V_s is the sliding velocity during rolling contact, P_e is Peclet number and S_r is the slide/roll ratio. Assuming that all the work done by the friction load is transformed into heat energy, the frictional heat generation is given as $Q_1(\tilde{x})=fV_sP_1(\tilde{x})$, $P_1(\tilde{x})$ being contact pressure and f being frictional coefficient. However in the present study, having specified the displacement shape of the roller, the contact pressure distribution $P_1(\tilde{x})$ is not given and $Q_1(\tilde{x})$ cannot be determined. In the previous study[9] for a single subsurface crack, $Q(x)$ was assumed to be Hertzian distribution being $Q_1(\tilde{x})=Q_0Q(x)$, $Q_0=fVS_rP_0$. In the present analysis, following the previous study[9], we assume that the frictional heat generation is given as:

$$Q_1(\tilde{x})=fVS_rP_0Q(x)=fVS_rP_0\sqrt{1-x^2} \quad (1)$$

The region outside the area of contact is assumed to be thermally insulated. Furthermore, it is assumed that the temperature distribution $T(x, y)$ is not affected by the presence of cracks. Thus, the thermal boundary conditions can be given as follows.

$$\left(\frac{\partial T}{\partial y}\right)_{y=0}=\begin{cases} fcVS_rP_0Q(x)/K_t, & |x|<1 \\ 0, & |x|>1 \end{cases} \quad (2)$$

$$(T)_{y\to-\infty}=0 \quad (3)$$

The mechanical boundary conditions on the surface and at infinity of the half-space are given as

$$\sigma_{xy}+f\sigma_{yy}=0,\ |x|<1 \quad (4)$$
$$\sigma_{yy}+i\sigma_{xy}=0,\ |x|>1 \quad (5)$$
$$U_{yy}/c=(x-x_0)^2/(2R)+y_0,\ |x|<1 \quad (6)$$
$$(\sigma_{pq})_{y\to-\infty}=0,\ (p, q=x, y) \quad (7)$$

where $\sigma_{pq}(p, q=x, y)$ are the stress components, U_{yy} is a vertical displacement and $i^2=-1$.

Assuming that crack face friction is neglected, the boundary condition along the cracks may be expressed as

$$(\sigma_{\xi_k\zeta_k})_{\zeta_k=0}=0,\ 0<\xi_k<l_k\ (k=1, 2) \quad (8)$$
$$(\sigma_{\zeta_k\zeta_k})_{\zeta_k=0}=0,\ \xi_k\in\xi_k^{op}\ (k=1, 2) \quad (9)$$

where $\xi_k^{op}(k=1, 2)$ is the crack face opening region of crack k.

We require continuity of displacements throughout the body except at the cracks and hence the condition for single valued of displacements is shown as

$$\oint(U_{xx}+iU_{yy})dz_k=0,\ (z_k=x_k+iy_k;\ k=1, 2) \quad (10)$$

where $\oint$ denotes the integration along a contour around the subsurface cracks.

3. Stress Analysis

In general, using Muskhelishivili's[12] complex stress function $\Phi(z)$, $\Psi(z)$ and a thermoelastic potential ω, thermal stresses and displacements are represented as:

$$\sigma_{yy}+\sigma_{xx}=2\{\Phi(z)+\overline{\Phi(z)}\}-2G_0\nabla^2\omega \quad (11)$$
$$\sigma_{yy}-\sigma_{xx}-2i\sigma_{xy}=2\{z\overline{\Phi'(z)}+\overline{\Psi(z)}\}-2G_0\left(\frac{\partial^2\omega}{\partial x^2}-\frac{\partial^2\omega}{\partial y^2}+2i\frac{\partial^2\omega}{\partial x\partial y}\right) \quad (12)$$
$$2G_0\left(\frac{U'_{xx}}{c}+i\frac{U'_{yy}}{c}\right)=\varkappa\Phi(z)-\overline{\Phi(z)}-z\overline{\Phi'(z)}$$

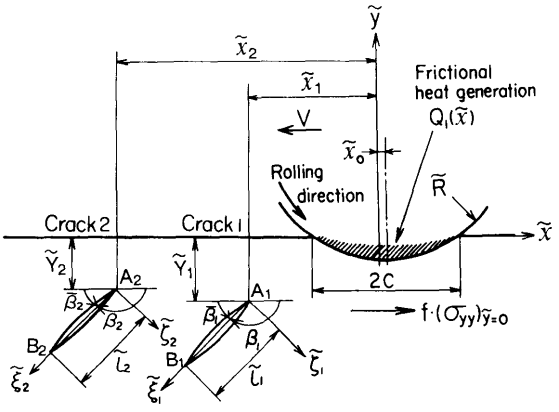

Fig. 1 Geometry and coordinate system

$$-\overline{\Psi(z)}+2G_0\left(\frac{\partial^2\omega}{\partial x^2}+i\frac{\partial^2\omega}{\partial x\partial y}\right) \tag{13}$$

$$\nabla^2\omega=\frac{1+\nu}{1-\nu}\alpha_0 T(x, y) \tag{14}$$

where primes denote differentiation with respect to $z(=x+iy)$ and $\nabla^2=\partial^2/\partial x^2+\partial^2/\partial y^2$, $\kappa=3-4\nu$. The thermal stresses and displacements for the half-space are represented as[13]:

$$\sigma_{yy}-i\sigma_{xy}=\Phi(z)-\Phi(\bar{z})+(z-\bar{z})\overline{\Phi'(z)}-2G_0\left(\frac{\partial^2\omega}{\partial x^2}+i\frac{\partial^2\omega}{\partial x\partial y}\right) \tag{15}$$

$$2G_0\left(\frac{U'_{xx}}{c}+i\frac{U'_{yy}}{c}\right)=\kappa\Phi(z)+\Phi(\bar{z})-(z-\bar{z})\overline{\Phi'(z)}+2G_0\left(\frac{\partial^2\omega}{\partial x^2}+i\frac{\partial^2\omega}{\partial x\partial y}\right) \tag{16}$$

First, the solution of the thermoelastic contact problem of a rigid roller with friction and arbitrarily distributed heat input on an uncracked half-space which satisfy the thermal and mechanical boundary conditions Eqs.(2), (3) and (4)-(7), are given by using the following stress function $\Phi_1(z)$ with Eqs. (15), (16) as a similar manner to the previous paper[9),14].

$$\Phi_1(z)=\frac{2iG_0(1+if)}{R(\kappa+1)}\{z-2\gamma-X(z)\}-\frac{2i\lambda(1+if)\cos(\pi\gamma)}{\pi(\kappa+1)}S_0(z)+\frac{\lambda\cos(\pi\gamma)}{\pi^2}\int_{-1}^{1}\{Q(u)-f\hat{Q}_1(u)/\sqrt{\pi P_e}\}\times S_1(z; u)du+\frac{i\lambda}{2\pi\sqrt{\pi P_e}}\int_1^\infty\frac{S_3(\nu)}{\nu-z}d\nu \tag{17}$$

where,

$$\lambda=fS_rH_0P_rG_0 \tag{18}$$

$$S_0(z)=\int_{-1}^{1}\frac{Q(t)}{X^+(t)}\left\{1+\frac{X(t)}{t-z}\right\}dt \tag{19}$$

$$S_1(z; u)=\int_{-1}^{1}\frac{1}{X^+(t)(t-u)}\left\{1+\frac{X(t)}{t-z}\right\}dt,\quad |u|<1 \tag{20}$$

$$S_3(\nu)=\int_{-1}^{1}Q(t)(t-\nu)^{-1.5}dt,\quad 1\le\nu\le\infty \tag{21}$$

$$X^+(t)=(1+t)^{0.5-\gamma}(1-t)^{0.5+\gamma} \tag{22}$$

$$X(z)=(z+1)^{0.5-\gamma}(z-1)^{0.5+\gamma} \tag{23}$$

$$\gamma=\frac{1}{\pi}\tan^{-1}\frac{(\kappa-1)f}{\kappa+1} \tag{24}$$

$$\hat{Q}_1(u)=\frac{\partial}{\partial u}\int_{-1}^{u}\frac{Q(\varepsilon)}{\sqrt{u-\varepsilon}}d\varepsilon \tag{25}$$

To account for the stress field caused by the cracks, we consider the problem of a pair of dislocations present at the points $z=z_{0k}$ ($z_{0k}=x_k+iy_k+\eta_k e^{-i\beta_k}$) in an infinite space. Then the dislocation density is defined as

$$\alpha_k=\frac{G_0}{i\pi c(\kappa+1)}\{[U_{\xi_k\xi_k}]+i[U_{\zeta_k\zeta_k}]\}e^{-i\beta_k} \tag{26}$$

where $\{[U_{\xi_k\xi_k}]+i[U_{\zeta_k\zeta_k}]\}$ represents the displacement jumps. This problem is solved by superposing the following complex stress functions with Eqs.(11)-(16) being $\omega=0$ as a similar manner to the previous paper[11].

$$\Phi_2(z)=\sum_{k=1}^{2}\left\{\frac{\alpha_k}{z-z_{0k}}\right\} \tag{27}$$

$$\Psi_2(z)=\sum_{k=1}^{2}\left\{\frac{\overline{\alpha_k}}{z-z_{0k}}+\frac{\alpha_k\overline{z_{0k}}}{(z-z_{0k})^2}\right\} \tag{28}$$

$$\Phi_3(z)=\begin{cases}-\bar{\Phi}_2(z)-z\bar{\Phi}_2'(z)-\bar{\Psi}_2(z), & \mathrm{Im}(z)<0\\ \Phi_2(z), & \mathrm{Im}(z)>0\end{cases} \tag{29}$$

$$\Phi_4(z)=-\frac{(1+if)}{2}\sum_{k=1}^{2}[(\alpha_k+\bar{\alpha}_k)\{F(z; z_{0k})-F(z; \bar{z}_{0k})\}-(z_{0k}-\bar{z}_{0k})\{\alpha_k G(z; z_{0k})+\bar{\alpha}_k G(z; \bar{z}_{0k})\}+(\alpha_k+\bar{\alpha}_k)\{1/X(z_{0k})-1/X(\bar{z}_{0k})\}+(z_{0k}-\bar{z}_{0p})\{\alpha_kX'(z_{0k})/X^2(z_{0k})+\bar{\alpha}_kX'(\bar{z}_{0k})/X^2(\bar{z}_{0k})\}] \tag{30}$$

where

$$F(z; \bar{z}_{0k})=\{1-X(z)/X(z_{0k})\}/(z-z_{0k}) \tag{31}$$

$$G(z; \bar{z}_{0k})=F(z; \bar{z}_{0k})-X(z)X'(z_{0k})/X^2(z_{0k})\}/(z-z_{0k}) \tag{32}$$

Thus, using the potentials Φ_2, Φ_3, Φ_4 and Ψ_2, we can obtain the stress field for a pair of dislocations α_k. Replacing the constant α_k with distributed dislocation density $\alpha_k(\eta_k)d\eta_k$ defined along the line ξ_k of each crack, the stress due to the cracks can be obtained by integration of η_k.

Superposing these results with the thermoelastic roller solution, the stress solution which satisfies the boundary conditions Eqs.(4)-(7). With substitution of these stresses into Eqs.(8)-(10), the following singular integral equations for α_k are obtained:

$$2e^{i\beta_k}\int_0^{l_k}\frac{\alpha_k(\eta_k)}{\xi_k-\eta_k}d\eta_k+\sum_{j=1}^{2}\int_0^{l_k}\{\alpha_j(\eta_j)\Gamma_{k,j}+\overline{\alpha_j(\eta_j)}\Lambda_{k,j}\}d\eta_j=(-\sigma^0_{\zeta_k\zeta_k}+i\sigma^0_{\xi_k\zeta_k})_{\Phi_1,\zeta_k=0},\quad (k=1, 2) \tag{33}$$

$$\int_0^{l_k}\alpha_k(\eta_k)d\eta_k=0,\quad (k=1, 2) \tag{34}$$

where

$$\Gamma_{k,j}=\sum_{r=3}^{4}\{\hat{\Phi}_r(z_k; z_{0j})+(1-e^{2i\beta_k})\overline{\Phi^*_r(z_k; z_{0j})}-e^{2i\beta_k}\hat{\Phi}_r(\bar{z}_k; z_{0j})+e^{2i\beta_k}(z-\bar{z})\overline{\Phi^{*\prime}_r(z_k; z_{0j})}\} \tag{35}$$

$$\Lambda_{k,j}=\sum_{r=3}^{4}\{\Phi^*_r(z_k; z_{0j})+(1-e^{2i\beta_k})\overline{\hat{\Phi}_r(z_k; z_{0j})}-e^{2i\beta_k}\Phi^*_r(\bar{z}_k; z_{0j})+e^{2i\beta_k}(z-\bar{z})\overline{\hat{\Phi}'_r(z_k; z_{0j})}\} \tag{36}$$

$$\hat{\Phi}_4(z_k; z_{0j})=-\frac{(1+if)}{2}\{F(z_k; z_{0j})-F(z_k; \bar{z}_{0j})-(z_{0j}-\bar{z}_{0j})G(z_k; z_{0j})+1/X(z_{0j})-1/X(\bar{z}_{0j})+(z_{0j}-\bar{z}_{0j})X'(z_{0j})/X^2(\bar{z}_{0j})\} \tag{37}$$

$$\Phi^*_4(z_k; z_{0j})=-\frac{(1+if)}{2}\{F(z_k; z_{0j})-F(z_k; \bar{z}_{0j})-(z_{0j}-\bar{z}_{0j})G(z_k; \bar{z}_{0j})+1/X(z_{0j})-1/X(\bar{z}_{0j})+(z_{0j}-\bar{z}_{0j})X'(\bar{z}_{0j})/X^2(\bar{z}_{0j})\} \tag{38}$$

$$\hat{\Phi}_3(z_k\,;\,z_{0j})=\begin{cases}-1/(z_k-\bar{z}_{0k}), & \mathrm{Im}(z)<0\\ 1/(z_k-z_{0k}), & \mathrm{Im}(z)>0\end{cases} \tag{39}$$

$$\Phi_3^*(z_k\,;\,z_{0j})=\begin{cases}-(z_k-\bar{z}_{0k})/(z_k-z_{0k})^2, & \mathrm{Im}(z)<0\\ 0, & \mathrm{Im}(z)>0\end{cases} \tag{40}$$

$$z_k=x_k+iY_k+\xi_k e^{-i\beta_k} \tag{41}$$

4. Numerical Calculations and Stress Intensity Factors

Equations (33), (34) was solved numerically using the piecewise quadratic method of Gerasoulis[15]. Each dislocation density $\alpha_k(\eta_k)$ are written as

$$\alpha_k(\eta_k)=\frac{G_0\hat{\alpha}_k(\hat{\eta}_k)}{R(1-\hat{\eta}_k)^{1/2}}e^{-i\beta_k},\quad \hat{\eta}_k=\frac{2\eta_k}{l_k}-1 \tag{42}$$

Let us the interval $[-1, 1]$ into $2N_k$ equal parts. We define the nodal points as $\hat{\eta}_{k,n}$ $(n=1\sim 2N_k+1)$, and use the Lagrange interpolation formula for three nodal points in the approximation. Setting the collocation points as $\bar{\hat{\xi}}_{k,r}=\hat{\eta}_{k,r}+1/2N_k$ $(r=1\sim 2N_k)$. Equations (33), (34) reduce to the simultaneous linear algebraic system of $(2N_1+2N_2)$ equations for $\hat{\alpha}_k(\hat{\eta}_{k,n})$. Using these solutions, the stress intensity factors at the crack tip A_k for crack k $(k=1, 2)$ are given as:

$$K_{\mathrm{I}}-iK_{\mathrm{II}}=-\frac{G_0}{R}\pi\sqrt{2cl_k}\,\hat{\alpha}_k(-1) \tag{43}$$

and at the crack tip B_k for crack k $(k=1, 2)$ are given as:

$$K_{\mathrm{I}}-iK_{\mathrm{II}}=\frac{G_0}{R}\pi\sqrt{2cl_k}\,\hat{\alpha}_k(1) \tag{44}$$

In carrying out the numerical calculations, it was necessary to determine iteratively the degree of crack opening for a given set of parameters. Iteration was performed under the condition of the absence of overlap of the material. First, the numerical solution was obtained for a completely open crack (ξ_k^{op}: $0<\xi_k<l_k$). The resulting crack opening displacement was checked by Eqs. (26), (42), and if overlap was found as $U_{\zeta_k\zeta_k}<0$, partial crack closure was approximated by setting $Re\{\hat{\alpha}_k(\hat{\eta}_{k,n})\}=0$ for that portion of the crack where overlap occurred. Then the procedure was repeated for the partially closed crack and results were verified. This method generally converged within three iterations. For the number of collocation points, a good accuracy was obtained for $n=10$.

Numerical calculations were carried out for horizontal parallel subsurface cracks ($\beta_1=\beta_2=180°$) with equal length ($l_1=l_2=0.1$), $P_e=100$, $H_0=1.0$[16),(17)] and $P_r=1.0$. The numerical results of stress intensity factors are shown for two cases of subsurface cracks which arranged in a series (Fig. 2) and arranged in a row (Fig. 3).

4.1 Subsurface cracks arranged in a series

In the present numerical results for Fig. 2, since the stress intensity factors at the both tips (A_1 and B_2 or A_2 and B_1) are almost equal, we show the results only at the crack tips A_1 and A_2. Figures 4 and 5 show the numerical results of stress intensity factors at the crack tip A_2 as functions of the contact location over complete loading cycle for $S_r=0.1$ and $S_r=0.7$ respectively. In these figures, mode I and II stress intensity factors K_{I}, K_{II} are shown for each values of $f=0.1, 0.7$, $Y_k=0.1, 0.5$ and $d_h=0.01, 0.5$. From these figures, we can see that the value of $(K_{\mathrm{I}})_{\max}$ is so small that it may be disregarded as compared to the value of $(K_{\mathrm{II}})_{\max}$. Therefore, the shearing mode crack growth seems to be predominant for horizontal subsurface crack. In Figs. 4 and 5, K_{II} attains a positive maximum at $x_2\fallingdotseq 0$ only for the case of $f=0.7$ and $Y_k=0.5$, however for

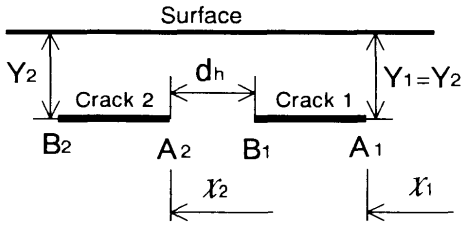

Fig. 2 Two subsurface cracks arranged in a series

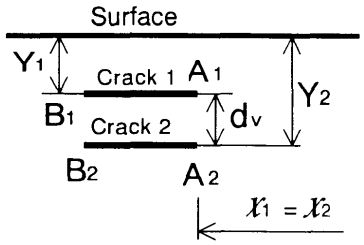

Fig. 3 Two subsurface cracks arranged in a row

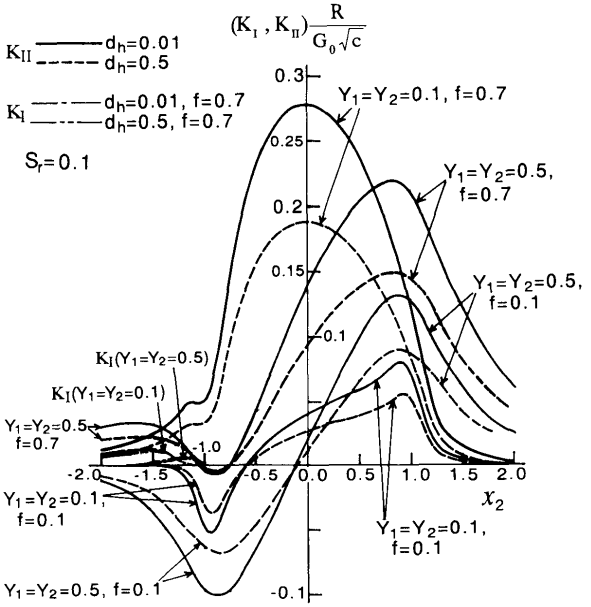

Fig. 4 Stress intensity factors K_{II} as a function of crack location for the case of $S_r=0.1$

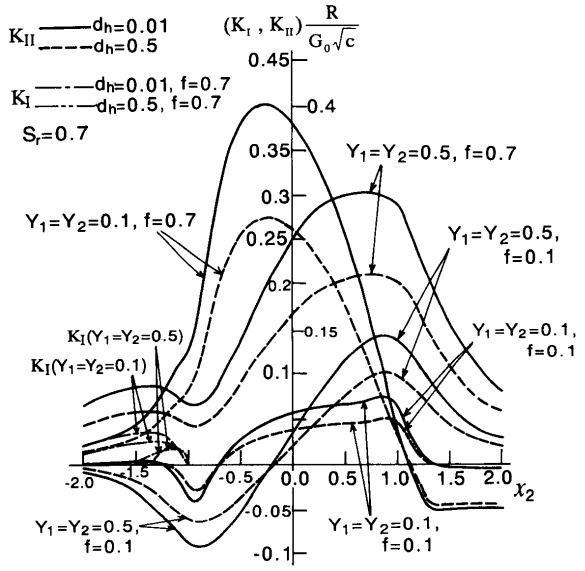

Fig. 5 Stress intensity factors K_{II} as a function of crack location for the case of $S_r=0.7$

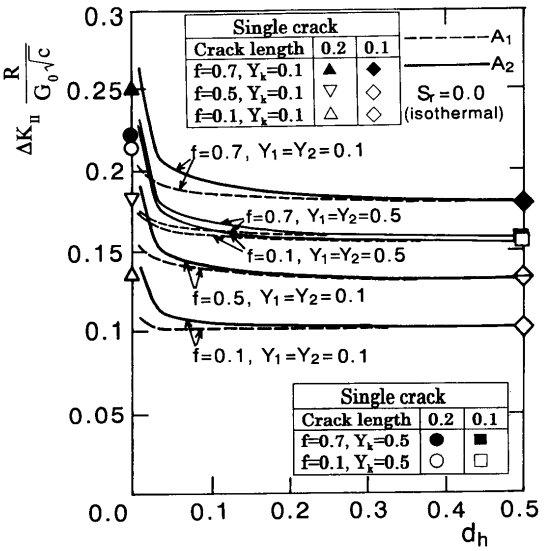

Fig. 6 Interference effects on ΔK_{II} with a decrease of d_h for isothermal case ($S_r=0$)

other cases, K_{II} attains a positive maximum at $x_2\fallingdotseq 1$ and a negative maximum at $x_2\fallingdotseq -1$. For the case of large frictional coefficient, the values of $(K_{II})_{max}$ for shallow crack ($Y_k=0.1$) are greater than those for deep crack ($Y_k=0.5$). Otherwise, for the case of small frictional coefficient, the values of $(K_{II})_{max}$ for deep crack ($Y_k=0.5$) are greater than those for shallow crack ($Y_k=0.1$). Comparing Fig. 4 ($S_r=0.1$) with Fig. 5 ($S_r=0.7$), the value of $(K_{II})_{max}$ for $S_r=0.1$ is greater than that for $S_r=0.7$ only for the case of $f=0.1$ and $Y_k=0.1$, however for another cases the values of $(K_{II})_{max}$ for $S_r=0.7$ are always greater than those for $S_r=0.1$. Moreover, in any cases, the values of $(K_{II})_{max}$ for $d_h=0.01$ are always greater than those for $d_h=0.5$ due to the mutual interference effect.

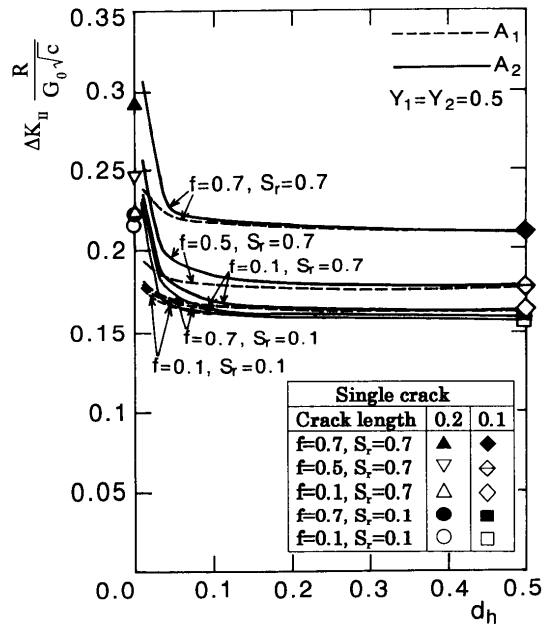

Fig. 7 Interference effects on ΔK_{II} with a decrease of d_h for the case of $Y_k=0.5$, $S_r=0.1$ and 0.7

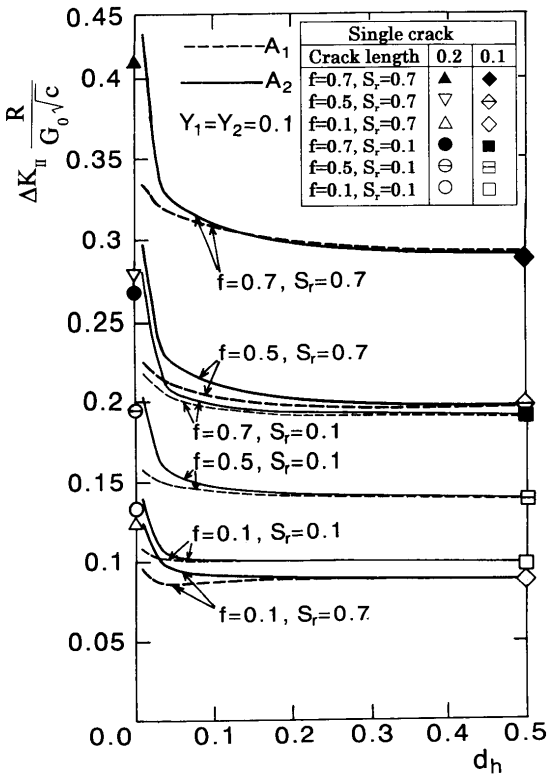

Fig. 8 Interference effects on ΔK_{II} with a decrease of d_h for the case of $Y_k=0.1$, $S_r=0.1$ and 0.7

Then, in order to investigate the mutual interference effects of the cracks, we evaluate the stress intensity factor range $\Delta K_{II}=(K_{II})_{max}-(K_{II})_{min}$ which is the important quantity in fatigue considerations, the results of which are shown in Figs. 6 - 8. In these figures, the values of ΔK_{II} at the crack tips A_1 and A_2

are shown as functions of the distance d_h between the cracks ($0.01 \leqq d_h \leqq 0.5$) for the isothermal case in Fig. 6 ($S_r=0$) and for the case of the existence of frictional heating in Fig. 7 ($Y_k=0.5$) and Fig. 8 ($Y_k=0.1$). From these figures, we can recognize the effect of mutual interference of the cracks; that is, the values of ΔK_{II} increase with a decrease of the distance d_h between the cracks. Especially, for $d_h<0.1\sim0.05$, the values of ΔK_{II} at the crack tip A_2 show a marked interference effect compared with ΔK_{II} at the crack tip A_1. In these figures, the results of single crack[9] are also shown by the symbols (◆◇■□) being the crack length $l=l_1=l_2=0.1$, and the symbols (▲△▽●○) being the crack length $l=l_1+l_2=0.2$ at $d_h=0$. As the distance d_h increase, the results of ΔK_{II} coincide with the results of the single crack which are shown by the symbols (◆◇■□). In fact, when two cracks go away from each other at a distance $d_h>0.5$, instead of those results of ΔK_{II} the results of single crack can be used. While, for the case of $d_h \leqq 0.01$, the results of ΔK_{II} at the crack tip A_2 are always greater than those results of single crack shown by the symbols (▲△▽●○), and the results of ΔK_{II} at the crack tip A_1 for $d_h=0.01$ are always smaller than the results of single crack which are shown by the symbols (▲△▽●○). Moreover, in order to investigate the mutual interference effects quantitatively, we consider the dimensionless quantities L_1, L_2 at the crack tip A_1, A_2, which represent the ratio of the value of ΔK_{II} for $d_h=0.01$ to the value for the single crack as:

$$L_k=(\Delta K_{II})_{d_h=0.01}/(\Delta K_{II})_{d_h=\infty},\quad (k=1:\ A_1,\ k=2:\ A_2) \tag{45}$$

At the crack tip A_2, the minimum value: $L_2=1.40$ for $S_r=0$, $f=0.1$, $Y_2=0.1$ (in Fig. 6) and the maximum value: $L_2=1.51$ for $S_r=0.7$, $f=0.7$, $Y_2=0.1$ (in Fig. 8), the mutual interference effect increase with an increase of thermal and frictional effects. However, in the present numerical examples, the degree of the increase is not so large as $1.4 \leqq L_2 \leqq 1.51$. At the crack tip A_1, the minimum value: $L_1=1.11$ for $S_r=0$, $f=0.1$, $Y_1=0.1$ (in Fig. 6) and the maximum value: $L_1=1.17$ for $S_r=0.7$, $f=0.7$, $Y_1=0.1$ (in Fig. 8), the mutual interference effect is smaller than that at the crack tip A_2 and the degree of the effect with thermal and frictional effects is also small as $1.11 \leqq L_1 \leqq 1.17$.

4.2 Subsurface cracks arranged in a row

As a numerical example for Fig. 3, the depth of the crack 2 is taken to be constant as $Y_2=0.5$. First, for the case of the crack distance $d_v=0.1$ and 0.01, the numerical results of the stress intensity factors K_I, K_{II} at the crack tip A_2 are plotted as functions of the contact location over a complete loading cycle in Fig. 9 for $S_r=0.1$, 0.7 and $f=0.1$, 0.7. From this figure, we can see that the value of $(K_I)_{max}$ is so small that it

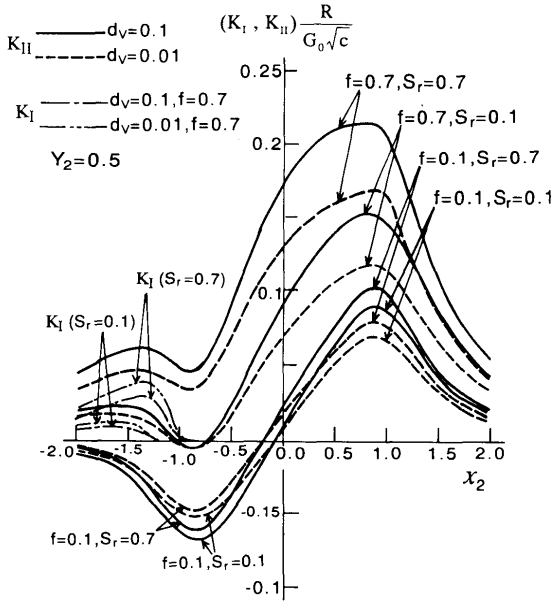

Fig. 9 Stress intensity factors K_{II} as a function of crack location for the case of $Y_2=0.5$

may be disregarded as compared to the value of $(K_{II})_{max}$. Therefore, the shearing mode crack growth seems to be predominant for horizontal subsurface crack. In any cases, the values of K_{II} attain a positive maximum at $x_2 \fallingdotseq 1$ and $(K_{II})_{max}$ increase with an increase of thermal and frictional effects, the values of $(K_{II})_{max}$ for $d_v=0.01$ are always smaller than those for $d_v=0.1$ due to the mutual interference effect.

Then, in order to investigate the mutual interference effects of the cracks, when the crack 1 approaches to crack 2 being constant depth $Y_2=0.5$, the numerical results of the stress intensity factor range $\Delta K_{II}=(K_{II})_{max}-(K_{II})_{min}$ at the crack tip A_2 of crack 2 are shown in Fig. 10 as functions of the distance d_v. In this figure, the results for the single crack[9] corresponding to the crack 2 are also shown by the broken line. In any cases, as the crack 1 approaches to the crack 2 from $d_v=0.4$, ΔK_{II} gradually increase and attains a maximum at $d_v \fallingdotseq 0.1$. The values of $(\Delta K_{II})_{max}$ are slightly larger than the values for the single crack. Furthermore, as the crack 1 approaches to the crack 2 for $d_v<0.1$, the values of ΔK_{II} rapidly decrease due to the mutual interference effect. Then, in order to investigate the mutual interference effects quantitatively, we consider the dimensionless quantities M_2 at the crack tip A_2, which represent the ratio of the value of ΔK_{II} for $d_h=0.01$ to the value for the single crack as:

$$M_2=(\Delta K_{II})_{d_v=0.01}/(\Delta K_{II})_{\text{single crack 2}} \tag{46}$$

From Fig. 10, the minimum value: $M_2=0.79$ for $S_r=0$, $f=0.1$ and the maximum value: $M_2=0.83$ for $S_r=0.7$, $f=0.7$, the mutual interference effect slightly decrease with an increase of thermal and frictional

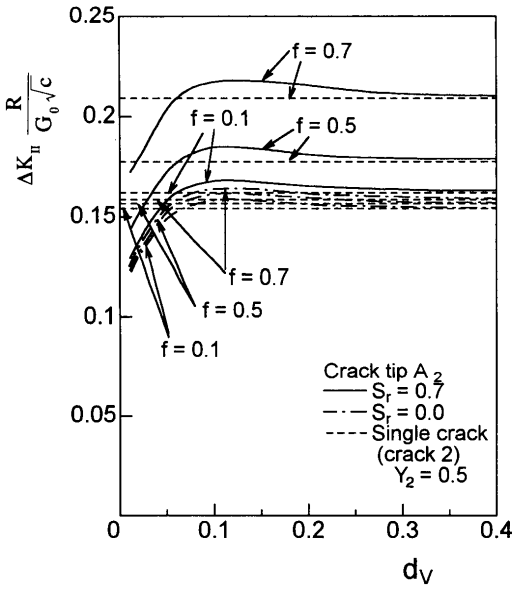

Fig. 10 Interference effects on ΔK_{II} of the crack tip A_2 with a decrease of d_v for $Y_2=0.5$, $S_r=0$ and 0.7

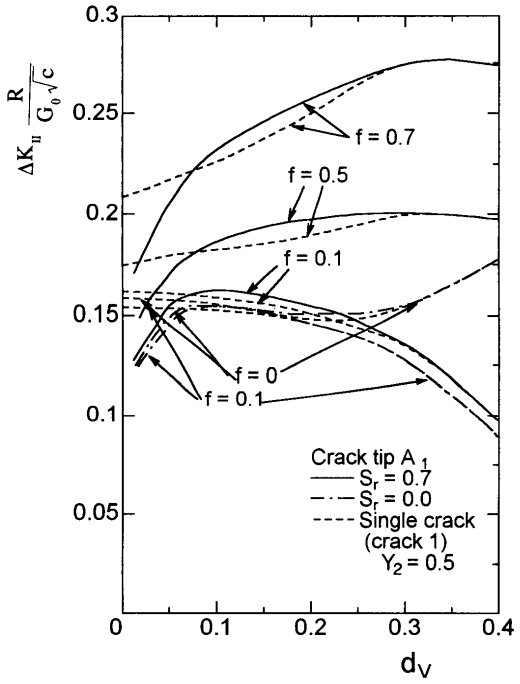

Fig. 11 Interference effects on ΔK_{II} of the crack tip A_1 with a decrease of d_v for $Y_2=0.5$, $S_r=0$ and 0.7

effects. However, in the present numerical examples, the degree of the effect is not so large as $0.79 \leqq M_2 \leqq 0.83$.

While, ΔK_{II} at the crack tip A_1 of crack 1 are shown in Fig. 11 as functions of the distance d_v for the crack 2 being constant depth $Y_2=0.5$. In this figure, the results for the single crack[9] corresponding to the crack 1 are also shown by the broken line. In any cases, when d_v is greater than 0.3, the results of ΔK_{II} are agree with the results of the single crack. For the case of $f=0.1$, as the crack 1 approaches to the crack 2 from $d_v=0.4$, ΔK_{II} gradually increase and attains a maximum at $d_v \fallingdotseq 0.1$. For the case of $f=0.5$ and 0.7, ΔK_{II} gradually decrease as a decrease of d_v. In any cases, for $d_v<0.07$, the values of ΔK_{II} are smaller than the values for the single crack. Furthermore, as the crack 1 approaches to the crack 2 for $d_v<0.07$, the values of ΔK_{II} rapidly decrease due to the mutual interference effect. Then, in order to investigate the mutual interference effects quantitatively, we consider the dimensionless quantities M_1 at the crack tip A_1, which represent the ratio of the value of ΔK_{II} for $d_v=0.01$ to the value for the single crack as:

$$M_1=(\Delta K_{II})_{d_v=0.01}/(\Delta K_{II})_{\text{single crack 2}} \quad (47)$$

From Fig. 11, as the minimum value: $M_1=0.80$ for $S_r=0$, $f=0.1$ and the maximum value: $M_2=0.83$ for $S_r=0.7$, $f=0.7$, we can see that the mutual interference effect is not so large in the same manner as crack 2.

5. Conclusions

We analyzed the stress intensity factors for a pair of subsurface cracks due to rolling/sliding contact by a rigid roller with frictional heat generation. From numerical examples of stress intensity factors for two parallel subsurface cracks with equal length arranged in a series or in a row, the following conclusions can be made within the present numerical examples.

(1) For the case of subsurface cracks arranged in a series, magnitudes of stress intensity factors at the inside crack tips increase with decreasing distance between the two inside crack tips due to mutual interference by the cracks. While, for the case of subsurface cracks arranged in a row, magnitudes of stress intensity factors decrease with decreasing distance between the two cracks due to mutual interference by the cracks. These interference effects on the increase or decrease of stress intensity factors are not greatly influenced by the frictional and thermal effects.

(2) When the dimensionless distance $d_h=0.01$ between the two inside crack tips for subsurface cracks arranged in a series, as the frictional coefficient and the frictional heat input increase, the magnitude of ΔK_{II} at the outside crack tips slightly increase from 1.11 times to 1.17 times as large as the magnitude of single crack, while the magnitude of ΔK_{II} at the inside crack tips increase from 1.40 times to 1.51 times as large as the magnitude of single crack.

(3) When the dimensionless distance $d_v=0.01$ between the two parallel subsurface cracks arranged in a row for the crack 2 being constant dimensionless depth $Y_2=0.5$, as the frictional coefficient and the frictional heat input increase, the magnitude of ΔK_{II} at the crack tips slightly increase from 0.80 times to 0.83 times as large as the magnitude of single crack,

and the interference effect on the crack 1 and that on the crack 2 are almost equal.

References

(1) Suh, N.P., The Delamination Theory of Wear, Wear, Vol. 44 (1977), pp. 1-16.

(2) Fleming, J.R. and Suh, N.P., Mechanics of Crack Propagation in Delamination Wear, Wear, Vol. 44 (1977), pp. 39-56.

(3) Rosenfield, A.R., A Fracture Mechanics Approach to Wear, Wear, Vol. 61 (1980), pp. 125-132.

(4) Hearle, A.D. and Johnson, K.L., Mode II Stress Intensity Factors for a Crack Parallel to the Surface of an Elastic Half-Space Subjected to a Moving Point Load, J. Mech. Phys. Solids, Vol. 33 (1985), pp. 61-81.

(5) Sheppard, S., Barber, J.R. and Comninou, M., Short Subsurface Cracks under Conditions of Slip and Stick Caused by a Moving Compressive Load, Trans. ASME, J. Appl. Mech., Vol. 52 (1985), pp. 811-817.

(6) Miller, G.R., A Preliminary Analysis of Subsurface Crack Branching under a Surface Compressive Load, Trans. ASME, J. Tribol., Vol. 110 (1988), pp. 292-297.

(7) Yu, M.M. and Keer, L.M., Growth of the Shell/Transverse Defect in Rails, Trans. ASME, J. Tribol., Vol. 111 (1989), pp. 648-654.

(8) Salehizadeh, H. and Saka, N., Crack Propagation in Rolling Line Contacts, Trans. ASME, J. Tribol., Vol. 114 (1992), pp. 690-697.

(9) Goshima, T. and Soda, T., Stress Intensity Factors of a Subsurface Crack in a Semi-Infinite Body Due to Rolling/Sliding Contact and Heat Generation, JSME Int. J., Ser. A, Vol. 40, No. 3 (1997), pp. 263-270.

(10) Goshima, T. and Kamishima, Y., Mutual Interference of Multiple Surface Cracks Due to Rolling-Sliding Contact with Frictional Heating, JSME Int. J., Ser. A, Vol. 37, No. 3 (1994), pp. 216-223.

(11) Goshima, T. and Kamishima, Y., Mutual Interference of Two Surface Cracks in a Semi-Infinite Body Due to Rolling Contact with Frictional Heating by a Rigid Roller, JSME Int. J., Ser. A, Vol. 39, No. 1 (1996), pp. 26-33.

(12) Muskhelishvili, N.I., Some Basic Problems in the Mathematical Theory of Elasticity, 4th ed. (1954), Noordhoff.

(13) Goshima, T. and Keer, L.M., Thermoelastic Contact between a Rolling Rigid Indenter and a Damaged Elastic Body, Trans. ASME, J. Tribol., Vol. 112 (1990), pp. 382-391.

(14) Dundurs, J., Mathematical Theory of Dislocations, (1975), p. 70, ASME Publication.

(15) Gerasoulis, A., The Use of Piecewise Quadratic Polynomials for the Solution of Singular Integral Equations of Cauchy Type, Comput. Math. Applics., Vol. 8 (1982), pp. 15-22.

(16) Azarkhin, A., Barber, J.R. and Rolf, R.L., Combined Thermal-Mechanical Effects in Frictional Sliding, Key Eng. Mater., Vol. 33 (1989), pp. 135-160.

(17) Hills, D.A. and Barber, J.R., Steady Motion of an Insulating Rigid Flat-Ended Punch over a Thermally Conducting Half-Plane, Wear, Vol. 102 (1985), pp. 15-22.